

High Quality GeSn Layer with Sn Composition up to 7% Grown by Low Temperature Magnetron Sputtering for Optoelectronic Application

Jiayin Yang¹, Huiyong Hu¹, Yuanhao Miao^{1*}, Linpeng Dong^{2,3}, Bin Wang¹, Wei Wang^{4,5}, Han Su¹, Rongxi Xuan¹, Heming Zhang¹

¹Key Laboratory of Wide-Gap Semiconductor Materials and Devices, School of Microelectronics, Xidian University, Xi'an 710071, China

²Guangdong Provincial Key Laboratory of Optical Fiber Sensing and Communications, Jinan University, Guangzhou, 510632, China

³Department of Optoelectronic Engineering, Jinan University, Guangzhou, 510632, China

⁴School of Physics and Electronic Information, Yunnan Normal University, Kunming, 650500, China

⁵Yunnan Key Laboratory of Opto-electronic Information Technology, Kunming, 650500, China

*Corresponding author: 15336118340@163.com

Abstract

In this paper, we have used magnetron sputtering to grow the high-quality GeSn layer on Ge (100) with Sn composition up to 7%. The crystallinity of the GeSn layer is pretty good, and the strain relaxation degree of the GeSn layer is evaluated to be approximately 50%. The root mean square (RMS) value is 0.8 nm, and the averaged TDDs in the GeSn layer is $8.7 \times 10^9 \text{ cm}^{-2}$, which is obtained from the rocking curve of GeSn layer along (004) plane. PL measurement result shows the significant optical emission from the deposited high-quality GeSn layer, which also means that magnetron sputtering is an optional way to achieve the higher Sn composition GeSn luminescent material. To verify whether our deposited GeSn can be used for optoelectronic devices, we fabricate the simple vertical p-i-n diode, and the room temperature current-voltage (I-V) characteristic was obtained. This result paves the way for future sputtered-GeSn optimization, which is critical for the optoelectronic application.

Keywords: GeSn layer; averaged TDD; magnetron sputtering; p-i-n diode

Introduction

Recently, GeSn alloys have the capability to become a direct bandgap material at an certain Sn composition of around 6%-10% [1-3], making it a possible candidate as the optical gain medium in group IV light source [4-6]. Besides, GeSn is also a complementary metal-oxide-semiconductor (CMOS) compatible optoelectronic material for Si photonics, which makes it more attractive. The epitaxial growth of high Sn composition GeSn with high material quality is challenging due to the solid solubility of Sn in Ge or Ge in Sn is less than 1%, and the smaller surface free energy of Sn than that of Ge makes Sn more likely immigrates to the surface of the GeSn film during epitaxial growth and thermal treatment [7-11]. So far, several techniques, such as CVD [12-14], MBE [15-17], and magnetron sputtering [18-22] have been employed to achieve the crystalline GeSn layers.

RPCVD has grown high-quality GeSn with Sn content up to 12.6% using Ge_2H_6 and SnCl_4 as precursors, which has led to the first demonstration of optical pumped GeSn laser [23]. The lasing of GeSn micro-disks with 16% Sn content has also achieved by using the same precursors [24]. At the same time, GeH_4 and SnCl_4 have also utilized to grown high-quality GeSn with Sn content up to 17%, which also contribute to the achievement of GeSn laser with the wavelength coverage of 2-3 μm and the lasing temperature of 180K[25]. Besides, high order Ge hydrides such as Ge_3H_8 and Ge_4H_{10} were also utilized to pursue high Sn content GeSn layers [26-28]. High-quality GeSn thin film with high Sn content (22.3%) was deposited on Sn graded GeSn buffer and optically pumped lasing has also been observed at the wavelength of 3 μm and lasing temperatures of 150K and 180K[29-31]. SiGeSn/GeSn/SiGeSn QW laser on Si with Sn content up to 14.4% has also been achieved, which features a higher maximum operating temperature of 90K and lower lasing thresholds of 25 and 62kW/cm² at 10 and 77K. MBE has grown high-quality GeSn, which contributes to the demonstration of GeSn light emitting diodes (LEDs) [33-36] and photodetectors[37-39]. However, GeSn laser has not been reported yet, which is mainly due to the lower Sn composition of the GeSn layer deposited by MBE.

Comparing with CVD and MBE, magnetron sputtering is also an alternative method to grow GeSn alloys. So far, only a few groups have grown crystalline GeSn alloys. High-quality GeSn layer was grown on a Ge (100) substrate by magnetron sputtering, which contributes to the first demonstration of GeSn p-i-n photodetectors [18]. High-quality SiGeSn/GeSn multiple quantum well (MQW) structure was also grown on Ge substrate by sputtering epitaxy, and Sn content of the GeSn layer is 6%, which contributes to the demonstration of GeSn photodetector [22]. In addition, crystalline GeSn thin films with high Sn content (28%) were also deposited on Sn graded GeSn buffer by sputtering epitaxy [20]. Our previous work has shown the deposition of GeSn on tensile-strained Ge buffer with low Sn content (3%), and room temperature photoluminescence spectrum has also been observed [21]. However, no room temperature photoluminescence spectrum and GeSn-based diode were reported for a higher Sn composition GeSn alloy deposited by this method. Besides, we propose a novel method to obtain the TDDs in GeSn layers from GeSn (004) rocking curves.

In this work, we have grown high-quality GeSn layer on Ge (100) substrate with Sn composition up to 7%. Room temperature optical emission from the GeSn layer is observed and averaged TDDs in the layer is also obtained from the rocking curve along (004) plane. To further verify the material quality of the film, we have fabricated simple vertical GeSn p-i-n diode.

Methods

Preparation of GeSn layers

GeSn epitaxial layer was deposited in physical vapor deposition (PVD) system manufactured by Kurt J. Lesker Corporation. High pure Ge target (99.999%) and Sn target (99.999%) were employed to deposit the GeSn layer on a Ge substrate. To prevent excess heating, the Ge target and Sn target were bonded to a copper baking plate. GeSn layer with Sn content up to 7% was deposited directly on Ge (100) substrate by magnetron co-sputtering, and Ge wafer was n-doped. At first, Ge wafer was cleaned by the running deionized water and etched with HF. A thin oxide layer

was prepared by dipping in a mixture of H₂O₂ and H₂O for a few seconds and the oxide layer was removed by dipping in HF. This procedure was repeated several times to ensure the removal of several atomic layers of Ge. After cleaning, the Ge wafer was loaded into PVD growth chamber and the chamber was pumped down to 10⁻⁶ mTorr as the base pressure. The substrate was heated to 160°C before the deposition of GeSn film. During the deposition, sputtering pressure was kept at 3mTorr by utilizing argon. The composition of Ge and Sn in the film was controlled by maintaining an RF power of 120W for the Ge target and varying the RF power of Sn target. The deposition rate is about 0.2-0.5nm/s, and the evaluated thickness of the GeSn layer is approximately 400nm.

Fabrication of simple GeSn diode

After the deposition of GeSn layer, B implant (dose of $4 \times 10^{15} \text{cm}^{-2}$ and energy of 40keV) was performed to dope the 400nm i-GeSn, followed by RTA in N₂ to activate the p-type dopant concentration. Then, the p-i-n diode was metallization processed and RTA treatment. The schematic cross section of the layer structure of the sample is shown in Fig.1 (a). In order to form a simple GeSn p-i-n diode, we have cut the sample into small pieces of 0.8mm×0.8mm square using laser slicing. Then, the typical I-V characteristic of the sample was measured by Keithley 4200 semiconductor characterization system parameter analyzer.

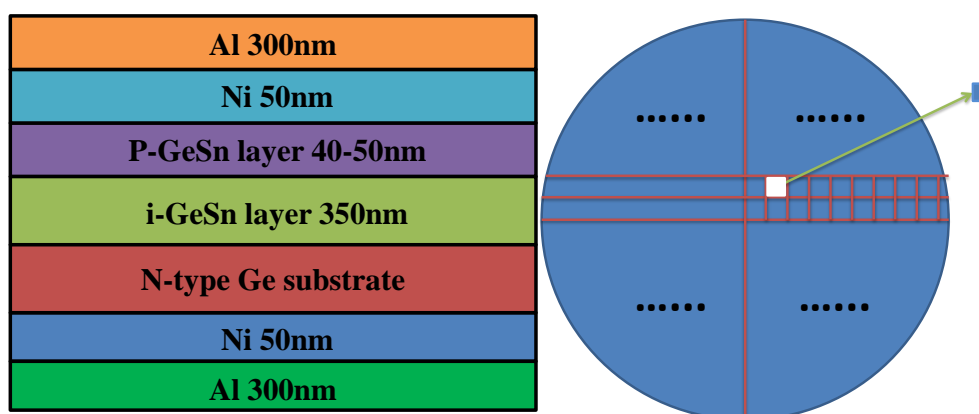


Fig.1 (a) The schematic cross section of the layer structure of the sample, (b) dicing diagram of the sample

Characterization method for GeSn layer

The crystallinity quality of the GeSn layer was determined by high-resolution

X-ray diffraction (HR-XRD) measurement. Sn composition of the GeSn layer was verified by energy dispersive spectrometer (EDS). The XRD 2theta- ω scans along (004) plane and (224) plane were accomplished. Rocking curve of GeSn (004) was also carried out to determine the averaged threading dislocation densities (TDDs) in the GeSn layer. PL was used to determine the band gap edge. PL setup consists of a Fourier transform infrared spectroscopy (FTIR), liquid nitrogen (LD₂) cooled InGaAs detector, 532nm continuous wave (CW) laser, and a grating monochromator.

Results and discussion

Crystallinity, Sn content, and strain of GeSn layer

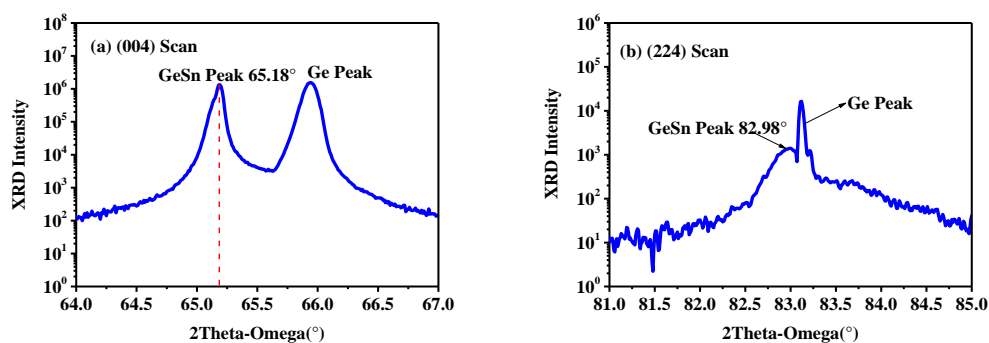


Fig.2 High resolution 2Theta-omega XRD scans of the GeSn alloy along (a) (004) plane, (b) (224) plane

The GeSn layer was grown on Ge (100) substrate by magnetron co-sputtering using high pure Ge target (99.999%) and Sn target (99.999%). The thickness of the GeSn layer was evaluated to be 400nm. High-resolution X-ray diffraction (HR-XRD) measurement was used to assess the crystallinity quality and Sn content of the epitaxial layer. Fig.2 (a) shows the XRD 2theta-omega (004) scan of the sample, in which the diffraction peak of GeSn and Ge can be seen. The peaks at 66° and 65.18° correspond to the Ge substrate and GeSn layer, respectively. The out-of-plane lattice constant of the GeSn layer was extracted from the following expression:

$$a_{Ge_{1-x}Sn_x}^{\perp} = \frac{2\lambda}{\sin \theta_{004}} \quad (1)$$

where λ represents the wavelength of Cu K1 ($\lambda=1.5406\text{\AA}$), and θ_{004} is the diffraction

peak of the GeSn layer along (004) plane. Hence, the out-of-plane lattice constant of the GeSn layer is calculated to be 5.721Å. Fig.2 (b) shows the XRD 2theta-omega (224) scan of the sample, in which the diffraction peak of GeSn and Ge can also be clearly seen. The peaks at 83.1° and 82.98° respond to the Ge substrate and GeSn layer, respectively. The in-plane lattice constant of the GeSn layer can be reckoned as:

$$a_{Ge_{1-x}Sn_x}^{\parallel} = \left[\frac{8}{\frac{1}{d_{224}^2} - \frac{16}{a_{Ge_{1-x}Sn_x}^{\perp 2}}} \right]^{1/2} \quad (2)$$

where d_{224} is the crystal spacing. For the XRD scan along (224), d_{224} can be calculated using the equation:

$$d_{hkl} = \frac{\lambda}{2 \sin \theta_{hkl}}, \quad (3)$$

Therefore, d_{224} of the GeSn layer is estimated to be 1.162Å. Substituting the value of d_{224} into eq.(2), the in-plane lattice constant of the GeSn layer is calculated to be 5.634Å.

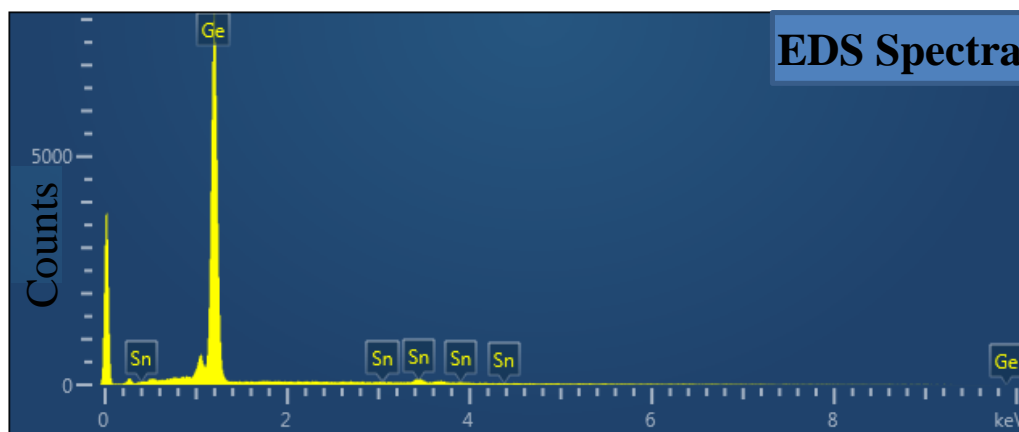


Fig.3 Surface energy dispersive spectrometer (EDS) spectra of the GeSn layer

To further determine the Sn content of the GeSn layer, we have carried out the surface EDS spectra of the GeSn layer. The spectra image was obtained from typical EDS analysis. **Fig. 3** shows that 7 primary peaks are formed at 0.4, 1.3, 3, 3.4, 4.4, 10, and 11keV. The peaks at 0.4, 3, 3.4 and 4.4keV match the spectral lines of Sn. Furthermore, the peaks at 1.3, 10, and 11keV match spectral lines of Ge. It was confirmed that Sn composition of the GeSn layer is estimated to be 7%. Based on the

lattice elastic theory, bulk lattice constant of GeSn (a_{bulk}) can be obtained using the following equation:

$$\frac{a_{\perp} - a_{bulk}}{a_{//} - a_{bulk}} = -\frac{2C_{12}}{C_{11}} \quad (4)$$

where a_{\perp} is the out-of-plane lattice constant of the GeSn layer, $a_{//}$ is the in-plane lattice constant of the GeSn layer, C_{11} and C_{12} are the elastic coefficient. Besides, there is a relationship between C_{11} , C_{12} , and the Sn composition of the GeSn [40]:

$$\frac{C_{11}}{C_{12}} = 0.3738 + 0.1676x - 0.0296x^2 \quad (5)$$

We can first substitute the Sn composition (7) obtained from EDS into Eq.(5), and the value of C_{11}/C_{12} is calculated to be 0.0966. a_{bulk} can also be calculated using the in-plane lattice constant of the GeSn layer, out-of-plane lattice constant of the GeSn layer, and the value of C_{11}/C_{12} (0.0966). The bulk lattice constant of the GeSn is calculated to be 5.707Å.

Therefore, the relaxation degree can be demonstrated as:

$$R = \frac{a_{//}^{GeSn} - a_{\perp}^{GeSn}}{a_{bulk}^{GeSn} - a^{Ge}} \quad (6)$$

where a^{Ge} is the lattice constant of the Ge ($a^{Ge} = 5.658\text{Å}$), a_{\perp} is the out-of-plane lattice constant of the GeSn, $a_{//}$ is the in-plane lattice constant of the GeSn, and a_{bulk} bulk lattice constant of GeSn. Finally, the relaxation degree of the GeSn layer is evaluated to be approximately 50%.

Averaged TDDs in GeSn layer

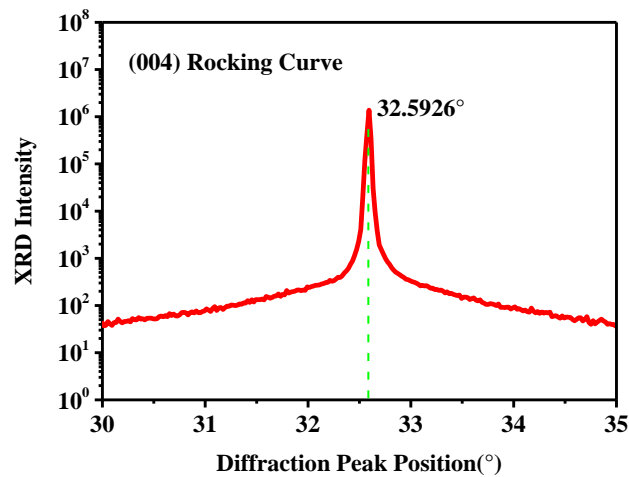


Fig.4 Rocking curve of GeSn layer along (004) plane

By now, transmission electron microscope (TEM) and etching pit density (EPD) have been utilized to evaluate the TDDs in GeSn layers. However, it is difficult to determine the dislocation density of the material using EPD when the dislocation density is more than 10^6cm^{-2} . Moreover, TEM also has its regional limitation because TEM can only obtain the TDDs of the material in a small region. So, we evaluate the TDDs of GeSn layer by rocking curve. High-resolution x-ray diffraction (HR-XRD) patterns are recorded on a Phillips X'Pert diffractometer operating at 40 mA and 40 kV with using Cu $K\alpha_1$ radiation. From our previous report [41], the intrinsic FWHM of strained GeSn can be described as:

(6)

where r_c is the radius of the electron, λ is the wavelength of the X-ray, θ is the Bragg angle, $|F_{hkl}|$ is the reflection structure factor for the (hkl), a_0 is the lattice constant of the bulk GeSn, and ϕ is the angle between the crystal surface and the diffracting planes.

The reflection structure factor for the GeSn (004) are all $64f^2$, where f is the dispersion factor of an atom.

The FWHM broadening by the TDDs in GeSn layer can represented as:

$$\beta_{TDD}^2 \approx \beta_m^2(hkl) - \beta_0^2(hkl) - \beta_d^2(hkl) \quad (7)$$

where β_m is the measured FWHM of the strained GeSn, β_0 is the intrinsic FWHM

of the strained GeSn, and β_d is the FWHM broadening by incident beam divergence of the instrument.

The averaged TDDs in the strained GeSn layer can be written as an empirical formula:

$$D = \beta_{TDD}^2 / 2\pi b^2 \ln 2 \quad (8)$$

The value of b is 0.4. The calculated values of β_m^2 , β_0^2 , β_d^2 , β_{TDD}^2 , and TDDs of GeSn layer are outlined in **Table I**. In addition, we compare the calculated TDDs with other results, which is closely consistent with the Ref TDDs.

Table I. Comparison of the calculated values of β_m^2 , β_0^2 , β_d^2 , β_{TDD}^2 , TDDs, and Ref TDDs for GeSn

	FWHM (arcsec)	β_m^2 (arcsec) ²	β_0^2 (arcsec) ²	β_d^2 (arcsec) ²	β_{TDD}^2 (arcsec) ²	Calculated TDDs (cm ⁻²)	Ref TDDs (cm ⁻²)
This work	627	395641	1324.32	419.068	393897.702	1.89×10^9	—
Ref [42]	2056	4227136	1324.32	419.068	4225392.61	2.03×10^{10}	2×10^{10}
Ref [43]	197	38809	1324.32	419.068	38065.612	1.78×10^8	6.5×10^7

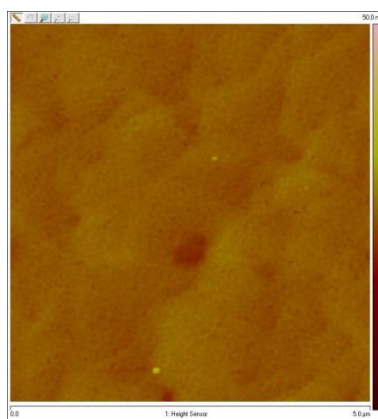


Fig.5 5μm×5μm AFM image of the GeSn layer deposited by magnetron sputtering

In order to determine the surface morphology of the GeSn layer, AFM measurement was performed. **Fig.5** shows the typical 5μm×5μm AFM image of the GeSn layer and RMS value of the GeSn sample was extracted from AFM scans. The as-grown GeSn layer shows a smooth surface and root-mean-squared (RMS) value is 0.8nm.

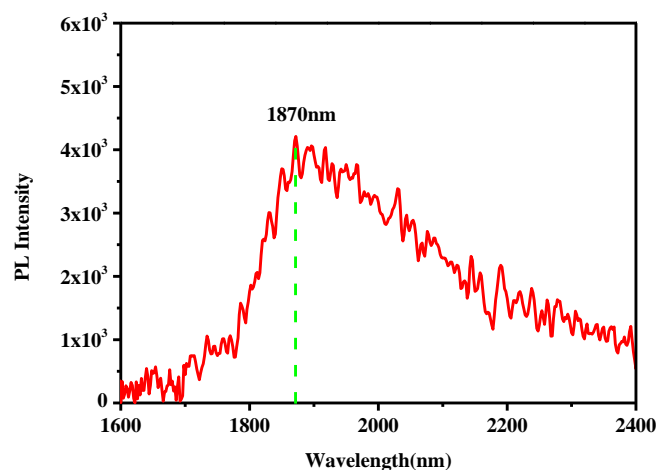


Fig.6 Room temperature PL spectra of the GeSn layer deposited by magnetron sputtering

The photoluminescence (PL) characterization was undertaken to examine the optical property of the GeSn layer. The PL measurement was excited by a continuous wave (CW) laser with 532nm wavelength. During the excitation of the laser, the laser beam was focused to be a 100 μ m spot and the power was modulated to be 500mW. The PL emission was collected (LN₂) by a Fourier transform infrared spectroscopy (FTIR), which is equipped with liquid nitrogen (LN₂) InGaAs detector. **Fig.6** shows the room temperature PL spectra of GeSn layer and the peak at 1870nm shows that GeSn layer is indirect bandgap material [1].

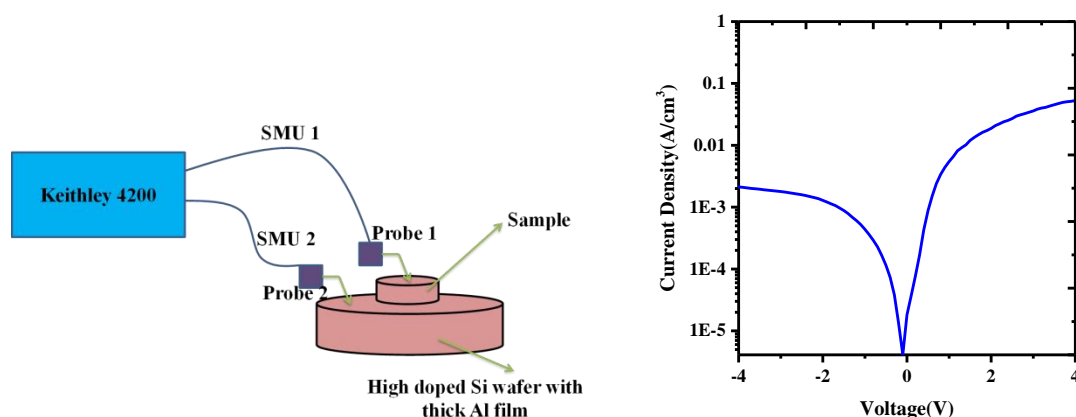


Fig.7 (a) Current-voltage (I-V) characteristic setup, (b) Room temperature current-voltage (I-V) characteristic of an 8mm \times 8mm square p-i-n diode with GeSn layer deposited by magnetron sputtering

Finally, the current-voltage (I-V) characteristic was carried out at room

temperature. The electrical property of the p-i-n diode was performed using a Keithley 4200 semiconductor characterization system parameter analyzer. **Fig.7 (b)** shows the typical I-V characteristic of an 8mm×8mm square p-i-n diode with the GeSn layer deposited by magnetron sputtering. The very high dynamic resistance may be attributed mainly to the fact that Si wafer and Ge substrate have a high series resistor. Ultimately, we can conclude that the sputter deposited GeSn layer has the great potential to be used for the fabrication of optoelectronic devices.

Conclusions

In summary, high-quality GeSn layer with Sn content up to 7% was successfully grown on the Ge (100) substrate via magnetron sputtering. The crystallinity of the GeSn layer is pretty good, and the strain relaxation degree in the layer is approximate 50%. The RMS value is only 0.8 nm, and the averaged TDDs in the GeSn layer is evaluated to be $8.7 \times 10^9 \text{ cm}^{-2}$ along (004) plane. PL measurement result shows the optical emission from the deposited high-quality GeSn layer. Besides, the fabricated vertical p-i-n device exhibit good room temperature current-voltage (I-V) characteristic. From the results, we conclude that sputter deposited GeSn have the potential to achieve high Sn composition GeSn layer with proper design, which is critical for the optoelectronic application.

Acknowledgement

This research is supported by the Natural Science Foundation of China (Grant No. 61704130 and No. 61474085), Science and Technology on Analog Integrated Circuit Laboratory (Grant No.6142802180206), Fundamental Research Funds for the Central Universities (Grant No.20101196823), and Science Research Plan in Shaanxi Province of China (Grant No.2019GY-019 and 2018JQ6064). Dr. Miao would also like to thank the support from the Fundamental Research Funds for the Central Universities, and the Innovation Fund of Xidian University.

References

[1] Ghetmiri S A, Du W, Margetis J, et al. Direct-bandgap GeSn grown on silicon

- with 2230 nm photoluminescence[J]. *Applied Physics Letters*, 2014, 105(15): 151109.
- [2] Stange D, Wirths S, von den Driesch N, et al. Optical Transitions in Direct-Bandgap $\text{Ge}_{1-x}\text{Sn}_x$ Alloys[J]. *ACS Photonics*, 2015, 2(11): 1539-1545.
- [3] Ryu M Y, Harris T R, Yeo Y K, et al. Temperature-dependent photoluminescence of Ge/Si and $\text{Ge}_{1-y}\text{Sn}_y/\text{Si}$, indicating possible indirect-to-direct bandgap transition at lower Sn content [J]. *Applied Physics Letters*, 2013, 102(17): 171908.
- [4] Oehme M, Werner J, Gollhofer M, et al. Room-temperature electroluminescence from GeSn light-emitting pin diodes on Si[J]. *IEEE Photonics Technology Letters*, 2011, 23(23): 1751-1753.
- [5] Zhou Y, Dou W, Du W, et al. Systematic study of GeSn heterostructure-based light-emitting diodes towards mid-infrared applications[J]. *Journal of Applied Physics*, 2016, 120(2): 023102.
- [6] Stange D, Von Den Driesch N, Rainko D, et al. Study of GeSn based heterostructures: towards optimized group IV MQW LEDs [J]. *Optics express*, 2016, 24(2): 1358-1367.
- [7] Li H, Cui Y X, Wu K Y, et al. Strain relaxation and Sn segregation in GeSn epilayers under thermal treatment[J]. *Applied Physics Letters*, 2013, 102(25): 251907.
- [8] Li H, Chang C, Chen T P, et al. Characteristics of Sn segregation in Ge/GeSn heterostructures[J]. *Applied Physics Letters*, 2014, 105(15): 151906.
- [9] Tsukamoto T, Hirose N, Kasamatsu A, et al. Investigation of Sn surface segregation during GeSn epitaxial growth by Auger electron spectroscopy and energy dispersive x-ray spectroscopy[J]. *Applied Physics Letters*, 2015, 106(5): 052103.
- [10] Wang W, Li L, Zhou Q, et al. Tin surface segregation, desorption, and island formation during post-growth annealing of strained epitaxial $\text{Ge}_{1-x}\text{Sn}_x$ layer on Ge (0 0 1) substrate[J]. *Applied Surface Science*, 2014, 321: 240-244.
- [11] Miao Y H, Hu H Y, Song J J, et al. Effects of rapid thermal annealing on crystallinity and Sn surface segregation of films on Si (100) and Si (111)[J]. *Chinese Physics B*, 2017, 26(12): 127306.
- [12] Margetis J, Mosleh A, Al-Kabi S, et al. Study of low-defect and strain-relaxed GeSn growth via reduced pressure CVD in H_2 and N_2 carrier gas[J]. *Journal of Crystal Growth*, 2017, 463: 128-133.
- [13] Grant P C, Dou W, Alharthi B, et al. UHV-CVD Growth of High Quality GeSn Using SnCl_4 : From Growth Optimization to Prototype Devices[J]. *arXiv preprint arXiv:1810.02523*, 2018.
- [14] Dou W, Alharthi B, Grant P C, et al. Crystalline GeSn growth by plasma enhanced chemical vapor deposition [J]. *Optical Materials Express*, 2018, 8(10): 3220-3229.
- [15] Gupta S, Chen R, Magyari-Kope B, et al. GeSn technology: Extending the Ge electronics roadmap[C] *Electron Devices Meeting (IEDM)*, 2011 IEEE International. IEEE, 2011: 16.6. 1-16.6.4.
- [16] Oehme M, Buca D, Kostecky K, et al. Epitaxial growth of highly compressively

- strained GeSn alloys up to 12.5% Sn [J]. *Journal of crystal growth*, 2013, 384: 71-76.
- [17] Yu K, Zhao Y, Li C, et al. The Growth of GeSn Layer on Patterned Si Substrate by MBE Method [J]. *ECS Transactions*, 2018, 86(7): 349-355.
- [18] Zheng J, Wang S, Liu Z, et al. GeSn pin photodetectors with GeSn layer grown by magnetron sputtering epitaxy[J]. *Applied Physics Letters*, 2016, 108(3): 033503.
- [19] Tsukamoto T, Hirose N, Kasamatsu A, et al. Formation of GeSn layers on Si (001) substrates at high growth temperature and high deposition rate by sputter epitaxy method[J]. *Journal of Materials Science*, 2015, 50(12): 4366-4370.
- [20] Zheng J, Liu Z, Zhang Y, et al. Growth of high-Sn content (28%) GeSn alloy films by sputtering epitaxy [J]. *Journal of Crystal Growth*, 2018, 492: 29-34.
- [21] Miao Y, Wang Y, Hu H, et al. Characterization of crystalline GeSn layer on tensile-strained Ge buffer deposited by magnetron sputtering [J]. *Materials Science in Semiconductor Processing*, 2018, 85: 134-140.
- [22] Zheng J, Wang S, Cong H, et al. Characterization of a $\text{Ge}_{1-x-y}\text{Si}_y\text{Sn}_x/\text{Ge}_{1-x}\text{Sn}_x$ multiple quantum well structure grown by sputtering epitaxy[J]. *Optics letters*, 2017, 42(8): 1608-1611.
- [23] Wirths S, Geiger R, Von Den Driesch N, et al. Lasing in direct-bandgap GeSn alloy grown on Si[J]. *Nature photonics*, 2015, 9(2): 88.
- [24] Reboud V, Gassenq A, Pauc N, et al. Optically pumped GeSn micro-disks with 16% Sn lasing at 3.1 μm up to 180 K[J]. *Applied Physics Letters*, 2017, 111(9): 092101.
- [25] Margetis J, Al-Kabi S, Du W, et al. Si-Based GeSn Lasers with Wavelength Coverage of 2–3 μm and Operating Temperatures up to 180 K[J]. *ACS Photonics*, 2017, 5(3): 827-833.
- [26] Grzybowski G, Jiang L, Beeler R T, et al. Ultra-low-temperature Epitaxy of Ge-based semiconductors and Optoelectronic structures on Si (100): Introducing higher order Germanes ($\text{Ge}_3\text{H}_8, \text{Ge}_4\text{H}_{10}$)[J]. *Chemistry of Materials*, 2012, 24(9): 1619-1628.
- [27] Grzybowski G, Beeler R T, Jiang L, et al. GeSn alloys on Si using deuterated stannane and trigermane: synthesis and properties [J]. *ECS Transactions*, 2013, 50(9): 865-874.
- [28] Xu C, Gallagher J D, Senaratne C, et al. CMOS compatible in-situ n-type doping of ge using new generation doping agents $\text{P}(\text{MH}_3)_3$ and $\text{As}(\text{MH}_3)_3$ (M= Si, Ge)[J]. *ECS Transactions*, 2015, 69(14): 3-15.
- [29] Dou W, Zhou Y, Margetis J, et al. Optically Pumped GeSn-edge-emitting Laser with Emission at 3 μm for Si Photonics[C]CLEO: Applications and Technology. Optical Society of America, 2018: AF1Q. 5.
- [30] Dou W, Zhou Y, Margetis J, et al. Optically pumped lasing at 3 μm from compositionally graded GeSn with tin up to 22.3%[J]. *Optics letters*, 2018, 43(19): 4558-4561.
- [31] Dou W, Benamara M, Mosleh A, et al. Investigation of GeSn Strain Relaxation and Spontaneous Composition Gradient for Low-Defect and High-Sn Alloy

- Growth[J]. *Scientific reports*, 2018, 8(1): 5640.
- [32] Margetis J, Zhou Y, Dou W, et al. All group-IV SiGeSn/GeSn/SiGeSn QW laser on Si operating up to 90 K [J]. *Applied Physics Letters*, 2018, 113(22): 221104.
- [33] Oehme M, Kostecki K, Arguirov T, et al. GeSn heterojunction LEDs on Si substrates[J]. *IEEE Photonics Technology Letters*, 2014, 26(2): 187-189.
- [34] Oehme M, Werner J, Gollhofer M, et al. Room-temperature electroluminescence from GeSn light-emitting pin diodes on Si[J]. *IEEE Photonics Technology Letters*, 2011, 23(23): 1751-1753.
- [35] Schwartz B, Oehme M, Kostecki K, et al. Electroluminescence of GeSn/Ge MQW LEDs on Si substrate[J]. *Optics letters*, 2015, 40(13): 3209-3212.
- [36] Gupta J P, Bhargava N, Kim S, et al. Infrared electroluminescence from GeSn heterojunction diodes grown by molecular beam epitaxy[J]. *Applied Physics Letters*, 2013, 102(25): 251117.
- [37] Su S, Cheng B, Xue C, et al. GeSn pin photodetector for all telecommunication bands detection[J]. *Optics express*, 2011, 19(7): 6400-6405.
- [38] Oehme M, Schmid M, Kaschel M, et al. GeSn pin detectors integrated on Si with up to 4% Sn[J]. *Applied Physics Letters*, 2012, 101(14): 141110.
- [39] Zhang D, Xue C, Cheng B, et al. High-responsivity GeSn short-wave infrared pin photodetectors[J]. *Applied Physics Letters*, 2013, 102(14): 141111.
- [40] Chang G E, Basu R, Mukhopadhyay B, et al. Design and modeling of GeSn-based heterojunction phototransistors for communication applications[J]. *IEEE Journal of Selected Topics in Quantum Electronics*, 2016, 22(6): 425-433.
- [41] Miao Y H, Hu H Y, Li X, et al. Evaluation of threading dislocation density of strained Ge epitaxial layer by high resolution x-ray diffraction [J]. *Chinese Physics B*, 2017, 26(12): 127309.
- [42] Tsukamoto T, Hirose N, Kasamatsu A, et al. Formation of GeSn layers on Si (001) substrates at high growth temperature and high deposition rate by sputter epitaxy method[J]. *Journal of Materials Science*, 2015, 50(12): 4366-4370.
- [43] Chang C, Li H, Huang S H, et al. Temperature-dependent electroluminescence from GeSn heterojunction light-emitting diode on Si substrate[J]. *Japanese Journal of Applied Physics*, 2016, 55(4S): 04EH03.